

See discussions, stats, and author profiles for this publication at: <https://www.researchgate.net/publication/40811552>

# Structure and Hydrogen-Bond Vibrations of Water Complexes of Azaaromatic Compounds: 7-(3'-Pyridyl)indole

ARTICLE in THE JOURNAL OF PHYSICAL CHEMISTRY A · MARCH 2010

Impact Factor: 2.69 · DOI: 10.1021/jp909409d · Source: PubMed

CITATIONS

10

READS

51

## 6 AUTHORS, INCLUDING:



**Gabriela Wiosna-Sałyga**

Lodz University of Technology

11 PUBLICATIONS 103 CITATIONS

SEE PROFILE



**Yevgeniy Nosenko**

Technische Universität Kaiserslautern

25 PUBLICATIONS 277 CITATIONS

SEE PROFILE



**Michał Kijak**

Instytut Chemii Fizycznej PAN

25 PUBLICATIONS 198 CITATIONS

SEE PROFILE



**J. Waluk**

Polish Academy of Sciences

257 PUBLICATIONS 3,690 CITATIONS

SEE PROFILE

# Structure and Hydrogen-Bond Vibrations of Water Complexes of Azaaromatic Compounds: 7-(3'-Pyridyl)indole<sup>†</sup>

Gabriela Wiosna-Sałyga,<sup>§</sup> Yevgeniy Nosenko,<sup>†,§</sup> Michał Kijak,<sup>§</sup> Randolph P. Thummel,<sup>‡,\*</sup> Bernhard Brutschy,<sup>†,\*</sup> and Jacek Waluk<sup>§,\*</sup>

*Institute of Physical and Theoretical Chemistry, University of Frankfurt, Max-von-Laue-Strasse 7, 60438 Frankfurt/M, Germany, Department of Chemistry, University of Houston, Houston, Texas 77204-5003, and Institute of Physical Chemistry, Polish Academy of Sciences, Kasprzaka 44, 01-224 Warsaw, Poland*

*Received: September 30, 2009; Revised Manuscript Received: December 4, 2009*

Complexes with water have been studied in the regime of supersonic jet isolation for 7-(3'-pyridyl)indole, a bifunctional molecule possessing hydrogen bond donor and acceptor groups. Two rotameric forms, syn and anti, are possible, of which only the former is able to form cyclic hydrogen bonds with protic solvents. Infrared-induced ion depletion spectroscopy was used to obtain vibrational patterns for 1:1 and 1:2 complexes in the hydrogen bond stretching region. The analysis of the spectra, supported by DFT calculations, revealed that for both stoichiometries the dominant forms correspond to cyclic, doubly or triply hydrogen-bonded species. The frequencies of  $\text{NH}\cdots\text{O}$ ,  $\text{OH}\cdots\text{N}$ , and  $\text{OH}\cdots\text{O}$  stretching vibrations were compared with the literature data to assess the strength of single vs multiple hydrogen bonds. Several new assignments and reassignments were proposed.

## 1. Introduction

The formation of an intermolecular hydrogen bond (HB) may lead to several effects with important structural, spectral, photophysical, and photochemical consequences.<sup>1–18</sup> For instance, opposite shifts of  $\pi\pi^*$  and  $n\pi^*$  excited states in complexes with protic partners may cause either enhancement or quenching of fluorescence, depending on the initial positions of the electronic levels in the isolated chromophore.<sup>4,17</sup> Quite often, intermolecular hydrogen bonds provide an efficient channel for energy dissipation, which results in an increase in the rate of internal conversion.<sup>7,13,16,19</sup> With regard to photochemistry, formation of hydrogen-bonded bridges consisting of water, alcohol, or ammonia may enable solvent-assisted excited state proton transfer in cases where the donor and acceptor are located too far from each other to make the direct, intramolecular process kinetically feasible.<sup>20–24</sup>

Solvent-assisted proton transfer usually involves more than one HB. In a molecule possessing both proton donor and acceptor groups, each of them can form a separate HB with the external partner, e.g., a protic solvent. Various structures of such complexes are possible. The same solvent molecule may simultaneously act both as a HB donor and as an acceptor, thus forming a solvate of 1:1 stoichiometry. Alternatively, two solvent molecules may separately bond to the donor and acceptor groups. In such 1:2 complexes, the solvent molecules may or may not form another HB between themselves; the former case leads to a cyclic, triply H-bonded structure. Leaving aside the entropy factor, the formation of three HBs should be energetically favorable. However, one has to keep in mind that, due to steric reasons, the geometries of the three HBs in a cyclic 1:2 complex are not optimal. In a series of papers devoted to structure and photophysics of systems revealing multiple

intermolecular HBs, we compared the characteristics of H-bonded complexes in condensed phases with the properties of the complexes isolated in supersonic jets.<sup>2,10,25–29</sup> A special class of bifunctional molecules consists of compounds for which the proton donor and acceptor groups are located in separate moieties, linked by a single bond. This class of molecules creates a possibility for the existence of two rotamers: (i) a syn form, with the donor and the acceptor on the same side; (ii) an anti species, with the two groups on the opposite sides. Both structures are able to form 1:2 complexes with water or alcohols; however, the cyclic species should be possible only for the syn species. In turn, since the two HBs are independent in the anti form, each bond can achieve the most favorable linear arrangement. The obvious question concerns the relative stability of these two H-bonded rotamers. Our studies, performed in solution for a series of structurally similar azaaromatic compounds, have shown that the syn form dominates, but the anti form is preferentially stabilized in polar and protic solvents. This stabilization was demonstrated by the finding that in nonpolar solvents only the syn rotamers were detected, whereas both syn and anti species were observed in alcohols.<sup>11,30</sup>

In this work, to determine the structural and HB characteristics of a bifunctional molecule with many possible solvation patterns, we focus on water complexes of 7-(3'-pyridyl)indole (7-3'PI) (Scheme 1). The calculations predict that the syn and anti form of this molecule should have nearly the same energies. Hydrogen bonding to water leads to complexes of different stoichiometries and structures, revealed by supersonic jet studies combined with resonance two-photon ionization and infrared ion depletion spectroscopy. The analysis of experimentally obtained and theoretically predicted vibrational patterns indicates that the dominant species for both 1:1 and 1:2 stoichiometries correspond to cyclic, doubly and triply hydrogen-bonded complexes, respectively.

In the second part of this work we provide some general remarks regarding the possibility and/or reliability of comparing characteristics of different kinds of hydrogen bonds (linear,

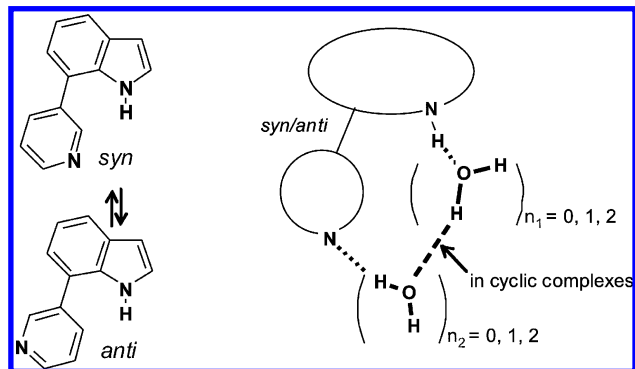
<sup>†</sup> Part of the "Benoît Soep Festschrift".

\* Corresponding author. E-mail: waluk@ichf.edu.pl.

<sup>†</sup> University of Frankfurt.

<sup>‡</sup> University of Houston.

<sup>§</sup> Polish Academy of Sciences.

**SCHEME 1: Syn and Anti Forms of 7-3'PI and Possible Structures of 1:1 and 1:2 Complexes with Water**


cyclic,  $\text{NH}\cdots\text{O}$ ,  $\text{OH}\cdots\text{N}$ ,  $\text{OH}\cdots\text{O}$ ) in a class of structurally similar molecules with one type of complexing solvent, water. For this purpose, we compiled all the available experimental data and then, to put all the systems on equal footing, recalculated all the complexes using the same model and basis set functions.

**2. Experimental and Computational Details**

The 7-(3'-pyridyl)indole was synthesized and purified according to the procedures described earlier.<sup>31</sup>

The setup for the resonant two-photon ionization (R2PI), laser induced fluorescence (LIF) excitation, and R2PI-detected infrared (IR/R2PI) measurements was described elsewhere.<sup>32</sup> To obtain H-bonded solute–solvent complexes, vapor of the protic solvent was added to the mixture of an inert carrier gas (helium) and the solute, which supersonically expanded into the vacuum through a modified high-temperature pulsed nozzle (General Valve Series 9). The temperature of the latter was maintained at about 390 K to ensure a sufficient and constant concentration of the gaseous solute. The partial pressure of the solvent was controlled by a gas mixing station. Cold molecules and clusters under collision-free conditions were then photoionized by UV laser pulses using the frequency-doubled tunable output of the Nd:YAG pumped dye laser (LPD3000, Lambda Physics). Fluorescence was collected at a right angle to both the molecular and the laser beams by a set of two lenses and imaged onto the entrance slit of a 250 mm spectrograph (Chromex 250IS), whose output was directed to a photomultiplier tube (Hamamatsu R4220) installed just behind a variable slit. The LIF spectra were only obtained for the isolated molecule, as the emission of the complexes should be very weak, due to efficient radiationless deactivation.<sup>26</sup> This was confirmed by weak ion signals of the complexes. R2PI spectroscopy was used to select a particular cluster size from the available size distribution in the beam, determined via its mass in a time-of-flight (TOF) mass spectrum.

The double-resonance IR/R2PI method<sup>33,34</sup> combines the structurally sensitive infrared (IR) vibrational predissociation spectroscopy with the mass- and species-selective R2PI technique. For measuring an IR spectrum in the ground electronic state, the IR laser pulses precede the UV laser pulses by about 100 ns. The two counterpropagating laser beams are focused and intersect the skimmed molecular beam at right angles in the first acceleration zone of the two-field linear TOF spectrometer. The IR laser pulses are generated by a home-built, injection seeded optical parametric oscillator (OPO) using  $\text{LiNbO}_3$  crystals. The laser pulse wavelength may be tuned in the range 2.5–3.5  $\mu\text{m}$  at a bandwidth of 0.2  $\text{cm}^{-1}$ . The typical output energy was about 3 mJ/pulse.

Ground state geometry optimizations and frequency calculations have been performed at the density functional level of theory (DFT). Hybrid functional, B3LYP, with a basis set including polarization and diffusion functions, 6-311+G(d,p), that is quite reliable in describing hydrogen bonds, has been used. In evaluating complexation energies, the basis set superposition error (BSSE) has been accounted for by using the counterpoise technique. All the ground state computations have been performed with the Gaussian 03 suite of programs.<sup>35</sup>

We have also tested another functional, M05-2X, recently recommended for calculations of noncovalent interactions, such as hydrogen bonding.<sup>36</sup> A perfect correlation was obtained between the binding energies calculated for 15 different water complexes using B3LYP and M05-2X. The energies computed using M05-2X were, on the average, 18% higher than those obtained using B3LYP. Also the vibrational frequencies calculated using the two functionals were correlated; the root-mean-square deviation between calculated and experimental values was slightly smaller for B3LYP. Since the frequencies are the main observables in this work, we use the computational results provided by B3LYP.

For excited state geometry optimizations, the time-dependent DFT method implemented in the Turbomole 5.0 package<sup>37,38</sup> has been chosen. The B3LYP functional and TZVP basis set have been used.

For stationary points, the Hessian matrix has been calculated and diagonalized to check whether the points correspond to minima.

**3. Results**

**3.1. DFT Calculations.** B3LYP/6-31G(d,p) and B3LYP/6-311+G(d,p) ground state geometry optimizations of the syn and anti rotamers of 7-3'PI yielded very similar energies, the syn being more stable by only 0.3 kcal/mol. This can be understood, since very similar values were obtained for the dihedral angles between the pyridyl and indole planes, about 45–50°. The calculated dipole moment of the syn form, 1.63 D (1.49 D with the 6-31G(d,p) basis set) was considerably smaller than that of the anti species, 2.98 (2.95) D.

Optimization of the  $S_1$  state resulted, for the isolated molecule, in a more planar geometry for both rotameric forms: as discussed below in more detail, the calculated dihedral angles between the indole and pyridine moieties were very similar.

The next step involved geometry optimization of 1:1 and 1:2 complexes of both rotameric forms with water. We considered the structures H-bonded in a cyclic fashion, as well as those with separate H-bonds to either indole or pyridine moieties. For 1:2 stoichiometry, the possibility of two water molecules bonded to the same center was also taken into account. The calculated binding energies and the HB-involving IR frequencies are presented in Tables 1 and 2, whereas the optimized structures are shown in Figures 1 and 2. Definitely, the most stable form corresponds to the syn species, either doubly (for 1:1) or triply (for 1:2 complexes) hydrogen-bonded in a cyclic fashion. Among the H-bonded anti species, the more stable are the ones with one or two waters attached to the pyridine nitrogen.

**3.2. Studies in Solutions.** We have previously reported biexponential fluorescence decays for 7-3'PI and its two isomers, 7-(2'-pyridyl)indole and 7-(4'-pyridyl)indole, in solutions at room temperature.<sup>39</sup> These studies have now been extended to include more solvents and temperature dependence of fluorescence. In polar solvents, the two components are of the order of several nanoseconds (e.g., about 4 and 8 ns in DMSO). This was interpreted as evidence of the presence of two forms. In

**TABLE 1: Binding Energies (kcal mol<sup>-1</sup>) of the Ground State Complexes of 7-3'PI with Water, Calculated at the B3LYP/6-311+G(d,p) Level<sup>a</sup>**

	1:1 stoichiometry			1:2 stoichiometry			
	<i>syn</i> -W <sub>1</sub>	<i>anti</i> -W <sub>1d</sub>	<i>anti</i> -W <sub>1a</sub>	<i>syn</i> -W <sub>2</sub>	<i>syn</i> -W <sub>11a</sub>	<i>anti</i> -W <sub>2d</sub>	<i>anti</i> -W <sub>2</sub>
$\Delta E^N$	-8.5	-6.8	-6.6	-22.0	-14.7	-16.0	-13.6
$\Delta E^B$	-7.5	-6.3	-5.5	-19.6	-12.8	-14.3	-11.9
$\Delta E^C$	-5.4	-3.4	-2.9	-14.9	-9.2	-10.1	-8.7

<sup>a</sup>  $\Delta E^N$  and  $\Delta E^B$  represent the binding energies without and with BSSE correction, respectively.  $\Delta E^C$  is the ZPVE-corrected  $\Delta E^B$ , with the scaling factor of 0.96 used for calculated frequencies.

**TABLE 2: Comparison of the Observed and B3LYP/6-311+G(d,p) Calculated Vibrational Frequencies (Scaled by 0.958) of the OH and NH Stretching Modes in the Complexes 7-3'PI:Water**

species	freq calc (cm <sup>-1</sup> )	freq exp (cm <sup>-1</sup> )	mode description <sup>a</sup>
isolated 7-3'PI	3513 ( <i>syn</i> ) 3515 ( <i>anti</i> )	3513	NH
1:1 Stoichiometry			
<i>syn</i> -W <sub>1</sub>	3382 3537 3729	3398 3555 3722	NH...O OH...N ss OH as free
<i>anti</i> -W <sub>2a</sub>	3358 3626		NH...O OH ss free
<i>anti</i> -W <sub>1d</sub>	3732 3513 3402 3720		OH as free NH OH...N ss OH as free
1:2 Stoichiometry			
<i>syn</i> -W <sub>2</sub>	3193 3302 3368 3723 3722	3160 3325 3420 3717	OH...N ss NH...O OH...O ss OH as free (as in water dimer) OH as free (ss in water dimer)
<i>syn</i> -W <sub>11a</sub>	3315 3536 3645 3657		NH...O OH...O ss OH...N as OH ss free
<i>anti</i> -W <sub>2d</sub>	3755 3216 3424 3515 3718 3726		OH as free OH...N ss OH...OH ss NH OH as free (water as donor to N) OH as free (water as donor to O)
<i>anti</i> -W <sub>2</sub>	3357 3401 3637 3722 3735		NH...O OH...N ss OH ss free (water as acceptor) OH as free (water as donor) OH as free (water as acceptor)

<sup>a</sup> ss, as = symmetric and antisymmetric stretch, respectively.

<sup>b</sup> Tentative assignment; see text for alternative explanation.

nonpolar *n*-hexane a monoexponential decay of 1.1 ns is observed. This single decay rate does not preclude the presence of both *syn* and *anti* species if their photophysical properties are not very different. In fact, the DFT and TDDFT B3LYP/TZVP calculations predict similar ground and excited state angles between the indole and pyridine moieties (49° and 50° for the *syn* and *anti* forms, respectively, in *S*<sub>0</sub>, 30° and 45° in *S*<sub>1</sub>), very similar *S*<sub>0</sub> → *S*<sub>1</sub> transition energies (32 470 vs 32 400 cm<sup>-1</sup>), and very similar oscillator strengths (0.12 vs 0.11). However, the two species are predicted to have different dipole moments in *S*<sub>1</sub> (8.93 vs 12.07 D), which should lead to a different stabilization in polar solvents. Calculations show that the dipole moment in *S*<sub>1</sub> increases with twisting. Thus, the angle between the indole and pyridine groups may change after excitation. The calculations predict that the oscillator strength of the *S*<sub>0</sub>–*S*<sub>1</sub> transition strongly decreases with the mutual twist of the two groups. The increase of both components of fluorescence decay in polar solvents with regard to the lifetime

measured in *n*-hexane suggests that both rotamers become more twisted in the excited state, albeit to a different degree. A similar result was obtained for 7-(4'-pyridyl)indole, an isomer of 7-3'PI with the pyridine nitrogen shifted from the meta to the para position with respect to the link with the indole moiety. Since this molecule has only one ground state rotameric structure, the values of the radiative rate constants could be determined in different solvents from the values of fluorescence quantum yields and decay times. The radiative rate was found to decrease by a factor of 4 upon passing from nonpolar to polar solvents, indicating that the molecule twists in *S*<sub>1</sub> in a polar environment.

In alcohols at 293 K, the two fluorescence decay components of 7-3'PI differ drastically, one being longer than in a nonpolar solvent (about 2 ns), whereas the other, dominant one, is significantly shorter (100 ps or less). This indicates the existence of at least two different types of complexes, of which one has access to an efficient channel of radiationless deactivation. Due to poor solubility in water, no solution studies were possible for this solvent. However, complexes with water could be investigated under the conditions of supersonic jet isolation.

**3.3. Investigations in Supersonic Jets. 3.3.1. Isolated Chromophore.** LIF and R2PI spectra of 7-3'PI (Figure 3) are very similar. The assignment of the 0–0 transition, which is very weak, at 32 416 cm<sup>-1</sup> is based on excellent agreement between the experimentally observed and calculated *S*<sub>1</sub> low frequency modes for the *syn* rotamer: experimental 67, 77, 105; calculated (TDDFT/TZVP, scaled by 0.956) 66, 76, 100 cm<sup>-1</sup>. These modes form long progressions and combinations, indicating significant geometry changes upon excitation to *S*<sub>1</sub>. Some weak bands are observed in the low frequency range, which can tentatively be assigned to another form, most probably the *anti* rotamer. However, further, more detailed experiments, are required to definitely solve the issue of the possible presence of more than one excited species.

**3.3.2. Mono- and Dihydrates of 7-(3'-Pyridyl)indole.** The presence of 7-3'PI:water complexes was manifested in the R2PI spectra by the appearance of very broad bands around 31 700 cm<sup>-1</sup> (1:1) and 30 700 cm<sup>-1</sup> (1:2) (Figure 4). Thus the complexes exhibit a red shift with respect to the 0–0 transition of the monomer and the absence of distinct vibrational structure in their absorption. Such behavior may have multiple origins, e.g., the occurrence of many ground state complexes with different geometries, as well as a short lifetime of the Franck–Condon excited state due to a rapid deactivation.

The IR/R2PI spectrum of the isolated monomer was recorded upon selective excitation at the vibronic transition located 153 cm<sup>-1</sup> above the origin. This spectrum possesses a single strong transition at 3513 cm<sup>-1</sup> due to the N–H stretch fundamental (Figure 5), which serves as a reference for the frequencies of the IR transitions in water complexes together with the OH stretching vibrations of a free water molecule:  $\nu_s = 3657$  cm<sup>-1</sup> and  $\nu_a = 3756$  cm<sup>-1</sup>.<sup>40</sup> As we further discuss quite strongly bound hydrates with rather decoupled OH stretchings of water,



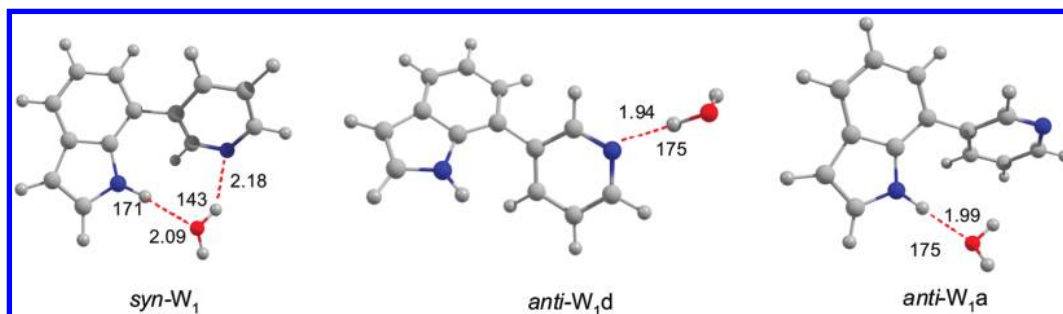


**Figure 1.** Three lowest energy B3LYP/6-311+G(d,p) optimized structures of the H-bonded complexes between 7-3'PI and one water molecule, with HB lengths (Å) and angles (degrees).

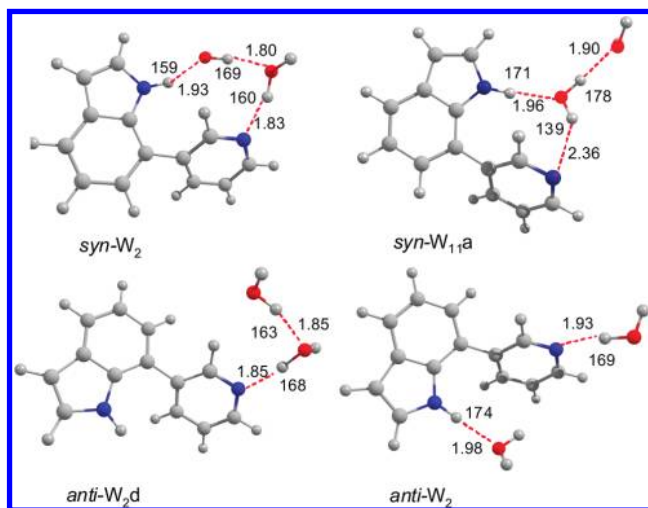


**Figure 2.** Four lowest energy B3LYP/6-311+G(d,p) optimized structures of complexes between 7-3'PI and two water molecules, with HB lengths (Å) and angles (degrees).

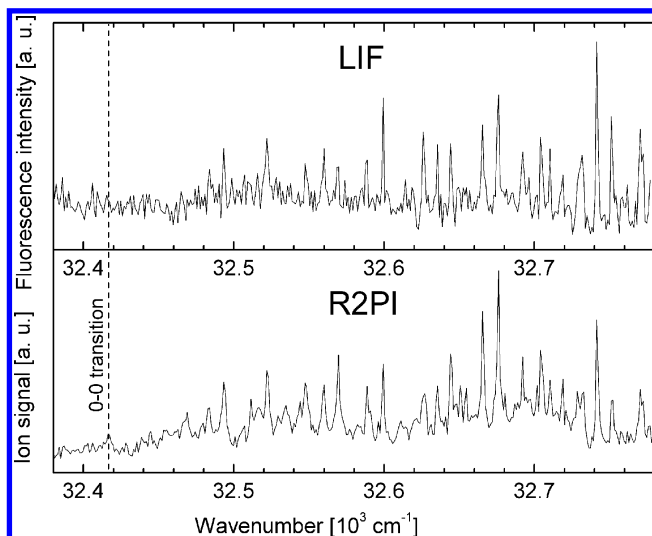


**Figure 3.** LIF excitation and one-color R2PI spectra of jet-cooled 7-3'PI.

the H-bonding induced frequency shifts are estimated with respect to a decoupled OH stretching of a free water molecule:  $(\nu_s + \nu_a)/2 = 3707 \text{ cm}^{-1}$ .

Figure 5 displays the IR dip spectrum of the 7-3'PI monohydrate measured by fixing the UV laser at  $31595 \text{ cm}^{-1}$  (see Figure 4), where the TOF spectra showed a large contribution from 1:1 complexes. This spectrum shows four dips at 3722, 3555, 3436, and  $3398 \text{ cm}^{-1}$ . The assignment can be made on the basis of DFT calculations and the experimental data for similar H-bonded systems.<sup>28</sup> The comparison of B3LYP/6-

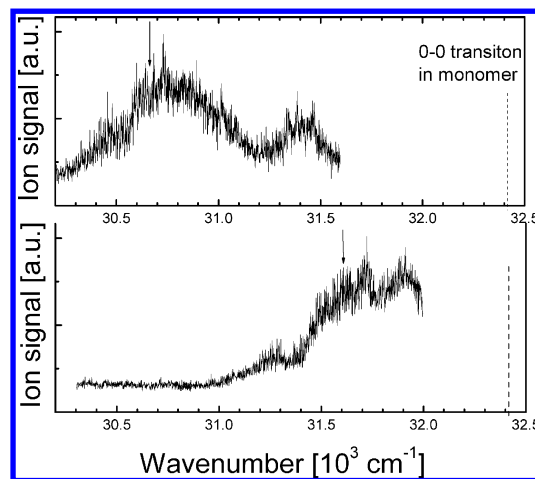


**Figure 4.** One-color R2PI spectra of the 1:1 (bottom) and 1:2 (top) complexes of 7-3'PI with water. The arrows indicate the wavelength of the UV laser selected for excitation in IR/R2PI experiments.

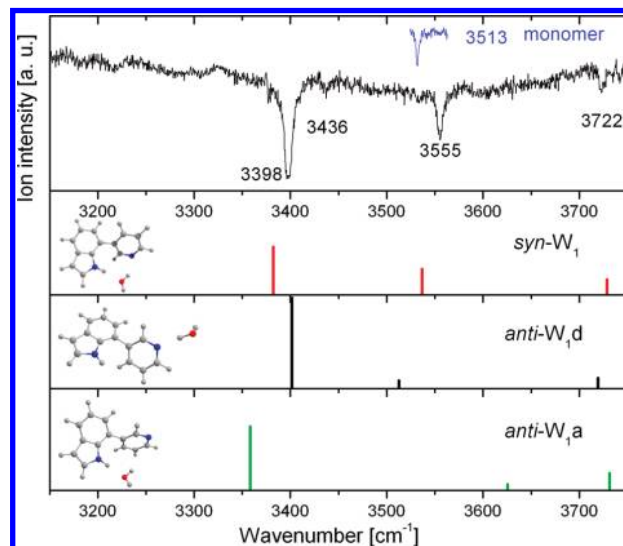


**Figure 5.** (Top) IR/R2PI spectra of the monomeric 7-3'PI and of the 1:1 water complexes. The vertical lines correspond to the calculated spectral positions and intensities in the three lowest energy complexes of 7-3'PI. The frequencies are scaled by a factor of 0.958, obtained as a ratio of the observed to the calculated frequency of the NH stretching in the monomer; this factor is similar to those typically used.

311+G(d,p) computed spectral positions of the vibrational bands of possible 1:1 complexes suggests that the spectrum is dominated by vibrations involved in a cyclic structure formed by the syn rotamer of 7-3'PI (*syn-W<sub>1</sub>*), predicted as the most stable one (Table 1 and Figure 1).

The highest frequency band observed at  $3722 \text{ cm}^{-1}$  is assigned to the free OH stretching vibration of water. This

**TABLE 3: Experimentally Obtained XH Frequency Shifts Caused by Hydrogen Bond Formation in Different Types of Hydrogen Bonded Complexes of Water with Various Azaaromatic Compounds**

	compound	stoichiometry/structure	$\Delta\nu(\text{NH}\cdots\text{O})$ ( $\text{cm}^{-1}$ )	$\Delta\nu(\text{OH}\cdots\text{N})$ ( $\text{cm}^{-1}$ ) <sup>a</sup>	$\Delta\nu(\text{OH}\cdots\text{O})$ ( $\text{cm}^{-1}$ ) <sup>a</sup>	ref
1	7-(3'-pyridyl)indole	1:1 cyclic	115	152		this work
		1:2 cyclic	188	547	287	this work
2	1 <i>H</i> -pyrrolo[3,2- <i>h</i> ]quinoline	1:1 cyclic	166	552		28
		1:2 cyclic	197	567	296	28
3	2-(2'-pyridyl)pyrrole	1:2 cyclic	151	541		51
4	7-azaindole	1:1 cyclic	109	338		44
		1:2 cyclic	409			44
			270	595	406	this work
		1:3 cyclic	435			44
			301	621	336, 391	this work
5	pyrrole	1:1 linear	83			47
6	indole	1:1 linear	89			46
		1:2 cyclic	123		219	46
7	carbazole	1:1 linear	91			43
		1:2 cyclic	127		217	43
		1:3 cyclic	212		263, 302	43
8	2-pyridone	1:1 cyclic	119			41
			159			50
		1:2 cyclic	253		370	41, 50
9	2-aminopyridine	1:1 cyclic	178	304		45
			90	392		this work
		1:2 cyclic	150	465	299	45
10	2-hydroxypyridine	1:1 cyclic		264		42
				334		50
		1:2 cyclic			335	50
11	7-hydroxyquinoline	1:1 linear		309		53
		1:2 cyclic		403	210	this work
		1:3 cyclic			346, 389	this work
12	pyridine	1:1 linear		286		54
13	4-(diethylamino)pyridine	1:1 linear		324		48
14	2-fluoropyridine	1:1 linear		176		55
		1:2 cyclic		305	208	55
		1:3 cyclic		374	246, 296	55

<sup>a</sup> With respect to the reference value of 3707  $\text{cm}^{-1}$ ; see text for details.

frequency is typical for a dangling OH stretching of a water molecule attached to the nitrogen atom of pyridine or bound in a cyclic complex.<sup>41–45</sup> The dip observed at 3555  $\text{cm}^{-1}$  may be assigned to the bound OH stretching vibration of water H-bonded to the pyridine nitrogen. The energy of this vibration is red-shifted by 152  $\text{cm}^{-1}$  with respect to the decoupled OH stretching of a free water. This shift is rather small, about half of that observed for the cyclic structure of the jet-cooled isolated 1:1 complexes of 7-azaindole, 2-aminopyridine, or 2-hydroxypyridine with water (cf. Table 3). It suggests that the geometry of the corresponding HB in 7-3'PI makes it weaker with respect to these other hydrates. Indeed, the calculations predict for 7-3'PI the OH–N angle of 143° and the N $\cdots$ H distance of 2.18 Å (Figure 1), both values indicating a weak hydrogen bond. Since this H-bond is not in the plane of the pyridine ring, the water may interact with its  $\pi$ -system. Typical  $\pi$  bound OH stretching of a water bridge shows up at higher frequencies: 3585  $\text{cm}^{-1}$  for indole–W<sub>2</sub>,<sup>46</sup> 3591 and 3598  $\text{cm}^{-1}$  for carbazole–W<sub>2</sub> and carbazole–W<sub>3</sub>, respectively.<sup>43</sup> So, the interaction causing the band at 3555  $\text{cm}^{-1}$  can be treated as intermediate between the OH $\cdots$ N and OH $\cdots$  $\pi$  H-bonds.

The most intense vibration at 3398  $\text{cm}^{-1}$  belongs to the hydrogen-bonded NH stretch fundamental, red-shifted by 115  $\text{cm}^{-1}$  with respect to this vibration in the monomer. A larger NH frequency shift was observed in cyclic 1:1 complexes of water with 1*H*-pyrrolo[3,2-*h*]quinoline (PQ, 166  $\text{cm}^{-1}$ ).<sup>28</sup> This is in line with different NH $\cdots$ O distances (calculated as 2.09 and 1.89 Å for 7-3'PI and PQ, respectively). On the other hand, pyrrole, indole, and carbazole monohydrates reveal shifts of 83,<sup>47</sup> 89,<sup>46</sup> and 91  $\text{cm}^{-1}$ ,<sup>43</sup> respectively. For these complexes, the

calculated hydrogen bonds are perfectly linear and shorter than in 7-3'PI (1.98 Å for all three, calculations carried out in this work). This comparison reveals the importance of effects other than pure geometrical factors, most probably the cooperativity between the two HBs, not possible in pyrrole, indole, and carbazole.

The weak band at 3436  $\text{cm}^{-1}$  can generally be treated in terms of either a Fermi resonance or a combination band or another hydrate isomer. A Fermi resonance is improbable, because water bending overtones, Fermi-resonant with the stretching fundamentals for the 2-aminopyridine and 4-(diethylamino)pyridine hydrates, are observed at 3343<sup>45</sup> and 3344  $\text{cm}^{-1}$ ,<sup>48</sup> respectively. The water bending frequency may increase with the strength of the H-bond donated by the water OH.<sup>49</sup> However, this is not the case. With 7-3'PI, water binds more weakly than with 2-aminopyridine or 4-(diethylamino)pyridine as revealed by the red shifts of the bound OH stretching vibrations. Weak bands above the strong fundamentals are sometimes assigned to combination vibrations.<sup>46,50</sup> Indeed, a mode of low frequency, 42  $\text{cm}^{-1}$ , is predicted by calculations. Alternatively, the band located at 3436  $\text{cm}^{-1}$  can be treated as a manifestation of the existence of clusters formed by the anti form of 7-3'PI, with water attached to the pyridine nitrogen. The 1:1 complex was photoionized via the broad UV absorption feature (Figure 3), where possible different isomers may overlap, thus limiting the isomer selectivity of the R2PI probe. The calculations predict that the binding energy for the anti structure is less favorable by 2.0 kcal/mol with respect to the syn complex (Table 1). The calculated vibrational transitions imply that the observed dip could belong to the H-bonded OH stretch; a weak intensity of

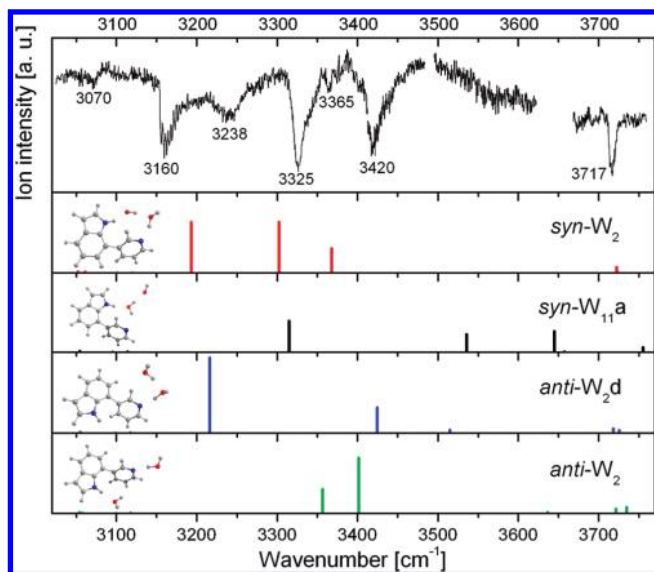


**Figure 6.** IR/R2PI spectra of 1:2 water complexes of 7-3'PI. The vertical lines correspond to the spectral positions and intensities in the spectra calculated for four lowest energy complexes; the scaling factor is 0.958.

the calculated transition may explain the lack of the trace of free NH stretch. The computational prediction for another possible 1:1 complex, the anti form with the water molecule hydrogen-bonded to the NH group (*anti-W<sub>1a</sub>*), suggests that such a structure should be more weakly bound (by 2.5 kcal/mol) in comparison with the most stable cluster. The IR/R2PI spectrum does not reveal the presence of such a type of complex under experimental conditions.

To measure the IR absorption spectra of the 1:2 water complexes, the UV probe was fixed to 30 667 cm<sup>-1</sup> (see Figure 4). This excitation energy was chosen to maximize the ion signal for the depletion experiment. The IR spectrum of 7-3'PI:W<sub>2</sub> (Figure 6) exhibits five main bands and several weaker features. Similarly as for 1:1 complexes, one can try, using the literature database and DFT calculations, to deduce the geometry or at least the number of different types of complexes observable under such conditions. It should be stressed that in the case of 1:2 complexes the measurements, repeated several times, have shown that the relative depletion of the ion signal should be treated with caution. The dip at 3717 cm<sup>-1</sup> is again attributed to the dangling OH stretching vibration of water. A weak, lowest frequency band at 3070 cm<sup>-1</sup> is most probably related to C–H stretch fundamentals. Among the rest of the observed transitions located at 3160, 3238, 3325, 3365, and 3420 cm<sup>-1</sup> one can look for the H-bonded NH indole stretching mode and the OH stretching of water involved in different types of HBs. On the basis of experimental data for similar H-bonded systems (2-(2'-pyridyl)pyrrole (PP)<sup>51</sup> and PQ<sup>28</sup>) and the results obtained for the 1:1 complexes, one could claim that such a depletion spectrum is indicative of the presence of cyclic 1:2 complexes in which the NH stretching vibration is located at 3325 cm<sup>-1</sup>, and the dips at 3160 and 3420 cm<sup>-1</sup> may be attributed to the OH stretch vibrations engaged in the HBs to pyridine and in the water dimer bridge, respectively. A pattern of three peaks, at 3140, 3310, and 3411 cm<sup>-1</sup>, similar both in frequencies and in relative intensities, was measured for PQ. Slight shifts of all three peaks to the red with respect to 7-3'PI indicate weaker HBs in the latter. This red shift is in agreement with the calculated geometries, which predict the OH...N, NH...O, and OH...O distances of 1.83, 1.93, and 1.80 Å for 7-3'PI, as

compared with 1.81, 1.90, and 1.77 Å for PQ. The calculated IR spectra of the *syn-W<sub>2</sub>* complex with the two water molecules forming a bridge between the indole and the pyridine ring, predicts three intense bands in the NH/OH stretch region, attributed to the H-bonded NH stretch (3302 cm<sup>-1</sup>), pyridine-bound OH (3193 cm<sup>-1</sup>), and the water dimer OH (3368 cm<sup>-1</sup>) stretchings. The comparison between the calculated and observed frequencies is given in Figure 6. The spectral analogies between 7-3'PI, PQ, and PP, as well as a fair matchup between experiment and calculation confirm the assignment of a dominant 7-3'PI:W<sub>2</sub> complex as *syn-W<sub>2</sub>*. We note that in this complex the two frequencies corresponding to NH...O and OH...N HB vibrations decrease significantly with respect to the values observed in the 1:1 cyclic form. This decrease indicates that both HBs become stronger in the 1:2 complex. This is confirmed by the calculated NH...O and OH...N distances, 2.09 and 2.18 Å for the 1:1 complex, and 1.93 and 1.83 Å for the 1:2 complex (Figures 1 and 2).

The spectrum corresponding to 1:2 complex reveals additional dips, which might indicate the presence of other isomers. Table 1 presents the calculated binding energies for a few of the most probable structures of 1:2 water complexes. Interestingly, when the dimer of water is attached to the NH indole group of the anti rotamer of 7-3'PI, the calculated structure converges to the cyclic *syn-W<sub>2</sub>*. The calculated vibrational transitions for the different clusters and the comparison with the experimental results do not allow one to definitively exclude the presence of any of them. It should be stressed that the observed dips are broad, so that in some cases two close-lying transitions may overlap. Keeping this in mind, the band at 3238 cm<sup>-1</sup> may be due a contribution from the *anti-W<sub>2d</sub>* complex. Alternatively, it may be due to the overtone of the water bending vibration. Moreover, an intense dip at 3420 cm<sup>-1</sup>, assigned to *syn-W<sub>2</sub>*, may also contain contributions from two different geometries of 1:2 complexes, *anti-W<sub>2</sub>* or *anti-W<sub>2d</sub>*. The most plausible assignment of the dip at 3365 cm<sup>-1</sup> is the combination of NH stretching (3325 cm<sup>-1</sup>) and a low-frequency mode in the dominant *syn-W<sub>2</sub>* complex. The calculations predict a vibration at 40 cm<sup>-1</sup>.

In summary, an unequivocal description of the IR/R2PI spectrum of the 1:2 complexes is not trivial. However, there is no doubt that the cyclic *syn-W<sub>2</sub>* complex is dominant under applied experimental conditions. This assignment seems reliable, not only due to the agreement between experimentally observed and computed IR transition frequencies and the analogy to PQ and PP but also because it corresponds to the structure with the lowest calculated energy (Table 1). The observed and calculated (B3LYP/6-311+G(d,p)) vibrational frequency shifts of the OH and NH stretching modes in complexes of 7-3'PI with respect to those of the free solvent molecules are summarized in Table 2.

#### 4. Discussion

The vibrational frequencies obtained for different types of microhydrates of 7-3'PI and for different types of hydrogen bonds, NH...O, OH...N, and OH...O allow us to discuss the influence of geometric and electronic factors on the HB strength. As a measure of the latter, one usually takes the red shift of the stretching vibrational frequency of the XH group engaged in the HB as a donor. In general, the more linear and shorter the bonding, the stronger it should be. This point is nicely illustrated by the analysis of the experimentally obtained frequencies and the calculated HB geometries of 1:1 and 1:2 complexes of 7-3'PI with water. As could be expected, higher frequencies are

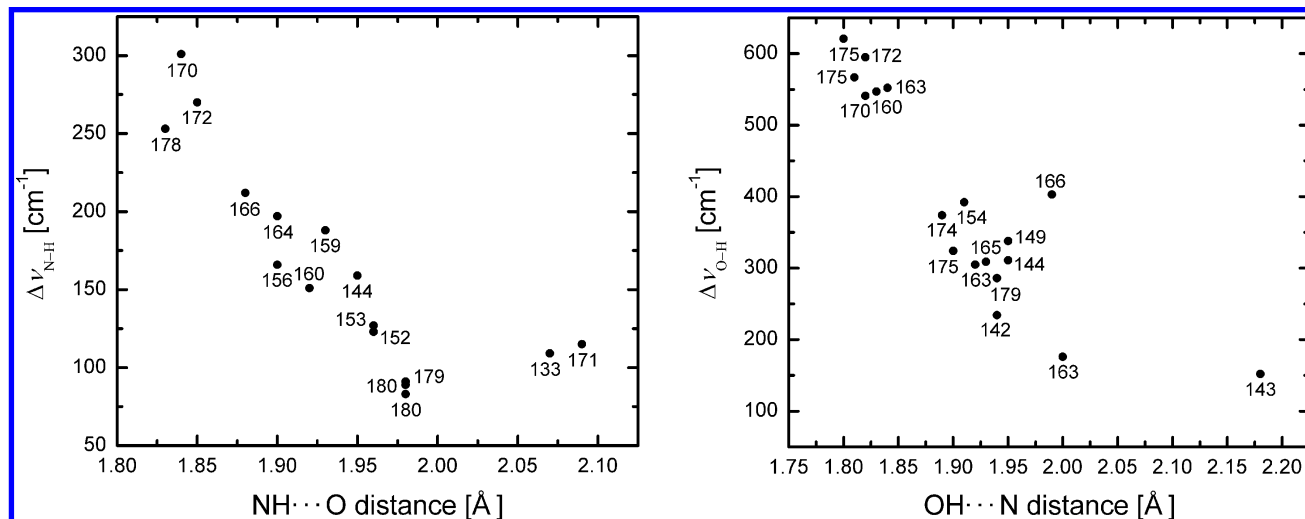


**Figure 7.** Correlation between the experimentally measured frequency red shifts of  $\text{NH}\cdots\text{O}$  (left) and  $\text{OH}\cdots\text{N}$  (right) HB stretching frequencies vs the calculated (B3LYP/6-311+G(d,p))  $\text{H}\cdots\text{O}$  and  $\text{H}\cdots\text{N}$  distances. The calculated values of the  $\text{NH}\cdots\text{O}$  and  $\text{OH}\cdots\text{N}$  angles (degrees) are also given. See Table 3 for the systems considered.

obtained for longer and less linear H-bonds of the 1:1 complex. Addition of the second water molecule alleviates the strain required for HB formation in cyclic species, which leads to shorter and more linear bonds and, in consequence, to lower vibrational frequencies. However, geometric constraints concerning linearity are not the decisive factor responsible for the HB strength. If they were, the lowest frequencies should be expected for noncyclic 1:1 complexes, which can readily form linear H-bonds. Inspection of the data obtained for water complexes of several structurally similar molecules show that this is not the case. In Table 3, we compile the experimental frequencies reported for numerous water complexes of azaaromatic compounds, of both the noncyclic type with linear H-bonds and the cyclic species. It can be seen that the frequency shifts caused by HB formation may be larger for cyclic complexes in spite of unfavorable geometry. For instance, formation of an HB between indole and water shifts the NH stretching frequency by  $89\text{ cm}^{-1}$ ; practically the same shift is observed for the 1:1 water complex of carbazole. On the other hand, for the cyclic 1:1 complexes of 7-3'PI or 7-azaindole with water, the corresponding values are larger, despite a less favorable HB geometry. One could argue that these data relate to different compounds, and so the comparison may not be appropriate. However, this is not the case if one considers that the same molecule can be H-bonded in several ways. In carbazole, for instance, water complexes of different stoichiometries have been found. The shift of the NH stretching frequency is smallest ( $91\text{ cm}^{-1}$ ) for the linear 1:1 complex, whereas it becomes much larger in the 1:2 cyclic complex ( $127\text{ cm}^{-1}$ ), even though the arrangement of the HB is no longer linear. As could be expected from the frequency shift values, the calculated  $\text{NH}\cdots\text{O}$  distance becomes smaller in the 1:2 complex, which again confirms the stronger HB. A general conclusion that can be drawn on the basis of comparison of the data obtained for cyclic and noncyclic complexes is that the cooperative effect caused by the formation of cyclic species prevails over the deviation from HB linearity required by the geometry. Naturally, the most favorable situation arises when the cyclic species can assume a linear or quasi-linear arrangement of HBs. In such circumstances, the values of both NH and, especially, OH shifts can become very large. Usually, more than one water or alcohol molecule is required, as is best illustrated by the cases of 7-3'PI, 7-azaindole, and PQ. For such strongly H-bonded complexes,

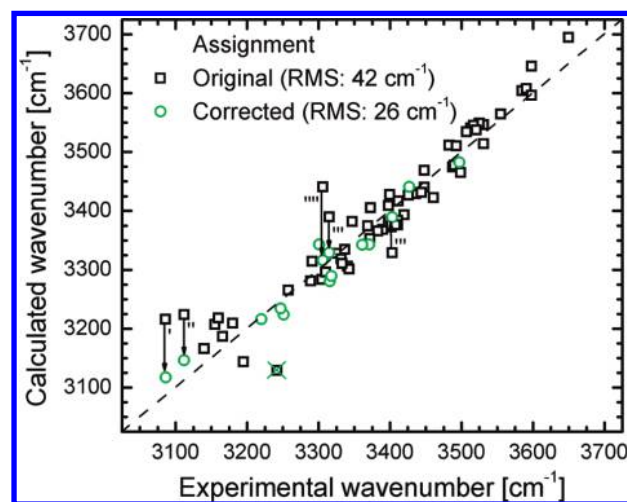


**Figure 8.** Comparison of experimental and calculated (B3LYP/6-311+G(d,p)) IR transition frequencies (scaled by 0.965). (—) (---) corrected assignments proposed for 7-azaindole (1:3 and 1:2), 2-aminopyridine (1:1), and 7-hydroxyquinoline (1:2), respectively. The crossed square (2-aminopyridine, 1:2) corresponds to a situation for which no band was observed, which could provide an alternative assignment. The root-mean-square (rms) errors for the previous and current assignments are also indicated.

the calculated normal modes show large mixing between the local NH and OH stretching modes. In other words, the cooperativity of HBs is expressed by the coupling of their vibrations.

The data from Table 3 are presented in Figure 7 in the form of plots of spectral shifts observed for intermolecular  $\text{NH}\cdots\text{O}$  and  $\text{OH}\cdots\text{N}$  hydrogen bond stretching frequencies vs the calculated  $\text{H}\cdots\text{X}$  distances. To put all the systems on equal footing, we have recalculated the geometry and vibration patterns of all the structures using the same DFT functional and basis set (B3LYP/6-311+G(d,p)). Comparison between the calculated and experimental frequencies is presented in Figure 8. The analysis of Figure 7 shows that even though the systems considered represent very different arrangements of hydrogen-bonded atoms, from linear to very nonlinear, the correlation is obvious. However, one can see that in some cases larger red shifts of the NH/OH stretching frequencies are observed despite longer and less linear hydrogen bonds. This is illustrated, e.g.,



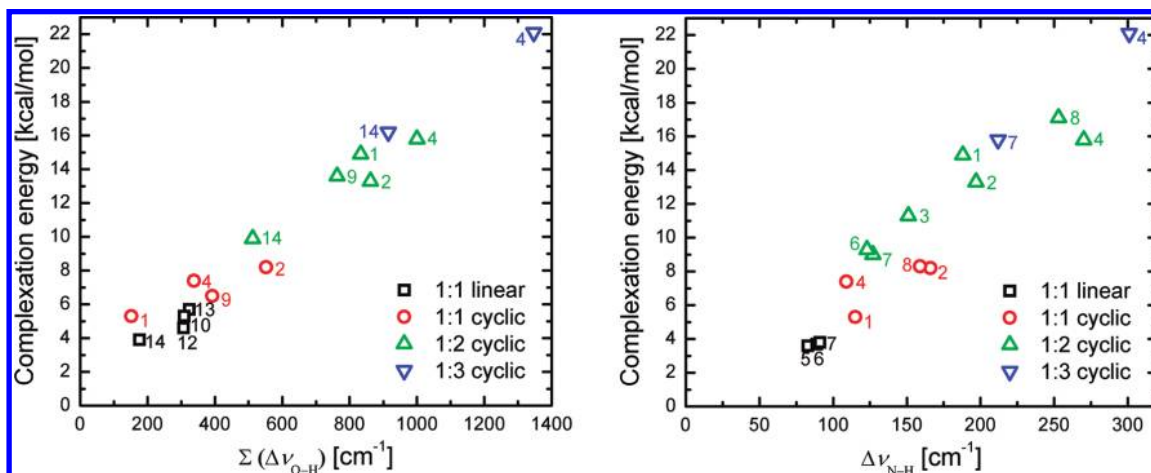


**Figure 9.** Correlation between the experimentally measured red shifts of  $\text{NH}\cdots\text{O}$  (right) and the sum of  $\text{OH}\cdots\text{N}/\text{OH}\cdots\text{O}$  (left) HB stretching frequencies vs the calculated (B3LYP/6-311+G(d,p)) complexation energies. See Table 3 for the systems considered.

by comparing the 1:1 cyclic complex of 7-azaindole with linearly H-bonded pyridine and 4-(diethylamino)pyridine monohydrates. Apparently, electronic effects due to cooperativity win over factors dictated by geometry of the H-bond. It should also be noted that steric factors not directly related to the HB length and angle may be important. For more flexible molecules, such as those where the HB donor and acceptor moieties are located in separate units linked by a single bond, the additional degrees of freedom may stabilize the interaction of the NH group with the acceptor water molecule, which simultaneously acts as an HB donor.

A correlation that should better encompass the different factors responsible for frequency shifts is that between the experimentally observed frequencies and the calculated complexation energies. We present such correlations in Figure 9, separately for the NH and OH stretches. For the latter, since more than one OH group is present for stoichiometries of 1:2 and higher, we used the sum of OH frequencies involved in the HB (a correlation involving only  $\text{OH}\cdots\text{N}$  frequencies was significantly worse). Both correlations are good; what is important is that they include systems of different geometries and different stoichiometries.

Due to the coupling of the HB-involving modes, the comparison of different molecules in terms of “pure”  $\text{XH}\cdots\text{Y}$  vibrations may not be appropriate. On the other hand, the influence of coupling could be removed if one correlates the sums of frequency shifts with the calculated H-bonding energies. Such a correlation is presented in Figure 10. Interestingly, while the correlation is good, it is only slightly better than those obtained separately for NH and OH stretching frequencies. This correlation indicates that a more accurate description of the HB may require taking into account modes other than NH and OH stretchings.

The very good correlation between the calculated and experimentally observed frequencies (Figure 8) suggests several new assignments and reassignments. For the 1:2 and 1:3 7-azaindole:water complexes, the rich vibrational structure did not allow for clear assignments. We propose to assign the peaks observed at 3251 and 3220  $\text{cm}^{-1}$  to NH stretches in the 1:2 and 1:3 complexes, respectively. The best candidates for the  $\text{OH}\cdots\text{N}$  stretches are the bands at 3112 and 3086  $\text{cm}^{-1}$ . Finally, for the water–water  $\text{OH}\cdots\text{O}$  vibrations, we suggest the band observed at 3301  $\text{cm}^{-1}$  in the 1:2 complex, and the bands at 3316 and 3371  $\text{cm}^{-1}$  in the 1:3 complex. Such assignments are supported not only by excellent correlation between the

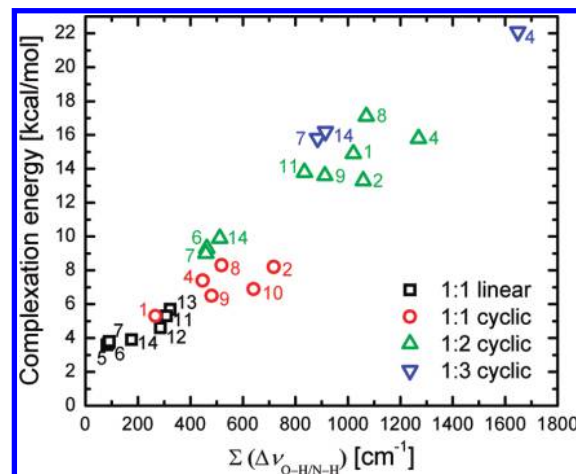


**Figure 10.** Correlation between the sums of experimental shifts in HB-related vibrational frequencies and the computed complexation energies. See Table 3 for the numbering.

calculated and observed values but also by the similarity of the shifts observed for similar geometries. For instance, the 1:2 stoichiometry is favored over the 1:1 ratio for 7-azaindole, whereas both 1:1 and 1:2 complexes are energetically favorable for PQ.<sup>28,52</sup> In this context, one can understand very similar and large shifts of  $\text{OH}\cdots\text{N}$  stretches observed for both types of PQ complexes, as well as in the 1:2 complex of 7-3'PI.

For 2-aminopyridine, we propose to assign the peaks at 3315 and 3403  $\text{cm}^{-1}$  to the OH and NH stretches, respectively. Tentative assignments are suggested for 1:2 and 1:3 complexes of 7-hydroxyquinoline. Finally, for 2-pyridone and 2-hydroxypyridine, the assignments made by Zwier and co-workers<sup>50</sup> seem preferred over the alternative ones.<sup>41,42</sup> Comparing the results of our B3LYP/6-311+G(d,p) calculations with previous computational data, we note that the introduction of diffuse functions leads to stronger coupling between the modes. This, in turn, results in more even intensity distribution, and in better agreement with experimental spectra. Such is the case, e.g., for 7-azaindole and 2-aminopyridine complexes.

Our data for 7-3'PI show that the cyclic complexes of syn character are favored in the regime of an isolated molecule. On the other hand, our studies in solutions revealed that the multiply H-bonded anti forms are preferentially stabilized in water or alcohols.<sup>11,30</sup> Apart from entropy factors, this difference between the jet and the condensed phase behavior can be understood, since for the latter, the alcohol/water molecules that form

independent (and thus linear) H-bonds to the donor and acceptor groups can also participate in other H-bonds with other solvent molecules. This solvent bonding is not the case for an isolated 1:2 complex. The only possibility for the latter to become energetically more stable is via formation of an additional  $\text{OH}\cdots\text{O}$  bond, i.e., to engage in a cyclic syn complex, even if it requires a less favorable, nonlinear HB geometry.

## 5. Conclusions

The results obtained for solutions show clearly that 7-(3'-pyridyl)indole exists in two rotameric forms. The specific and nonspecific interactions with the solvent may preferentially stabilize one of them. The studies of water solvation effects on jet-cooled 7-3'PI revealed that under experimental conditions the cyclic complexes of the syn rotamer are preferentially formed. These observations explain the efficient quenching of fluorescence of 7-3'PI in protic solvents in comparison with other members of the series of 7-pyridylindoles. The communication between the hydrogen bond centers seems to be the clue for a fast deactivation processes. It seems safe to assign the species revealing short fluorescence decay in alcohols to complexes solvated in a cyclic fashion. The cyclic complexes are efficiently deactivated in the  $S_1$ , via internal conversion. This rapid deactivation channel is not available in the anti rotamer of 7-3'PI. Actually, in isomeric 7-(2'-pyridyl)indole, for which the dominant syn form decays very rapidly due to intramolecular excited state proton transfer, a small amount of the solvated anti form could be detected in alcohol because its emission was not quenched. Finally, 7-(4'-pyridyl)indole, the third member of the series, reveals quenching by alcohols, but the process is less efficient than in 7-3'PI. It would be tempting to consider this molecule as a model for a bifunctional chromophore, which does not have a possibility to form cyclic water or alcohol complexes. Interestingly, however, energy optimizations for 1:2 water complexes converge to a cyclic H-bonded structure, even though the geometry of the HB between the pyridine nitrogen and water hydrogen is highly unfavorable. We plan to determine the structure of such complexes using the experimental techniques described in this work.

The main issue that requires further studies is the nature of rapid  $S_1$  deactivation in cyclic complexes. Initial computational studies suggest that the origin for this behavior is due to excited state proton transfer from water toward the pyridine nitrogen. A conical intersection was detected along the proton transfer path. The role of the NH group is to lower the energy of the proton transfer product, which is especially efficient in the cyclic species.

Finally, the results obtained in this work point out that the solution of 7-3'PI in alcohols is a very complex system, possibly containing a large number of differently solvated species, characterized not only by different structures but also by different photophysical characteristics. Each of the syn and anti rotamers can be hydrogen-bonded, in several ways, to a different number of protic solvent molecules. In previous studies of bifunctional compounds, we demonstrated that classical molecular dynamics simulations are able to reproduce the relative fractions of complexes of different stoichiometries. Such studies are now being initiated for 7-3'PI.

**Acknowledgment.** This work was supported by the grant N20414132/3545 from the Polish Ministry of Science and Higher Education. We acknowledge the computing grant G17-14 from the Interdisciplinary Centre for Mathematical and Computational Modeling of the Warsaw University. R.P.T.

thanks the Robert A. Welch Foundation (E-621) and the National Science Foundation (CHE) for support and Ajay Singh for the preparation of 7-3'PI. B.B. acknowledges the financial support by the Centre of Excellence Frankfurt.

## References and Notes

- (1) Chou, P.-T. *J. Chin. Chem. Soc.* **2001**, *48*, 651.
- (2) Waluk, J. *Acc. Chem. Res.* **2003**, *36*, 832.
- (3) Chai, S.; Zhao, G. J.; Song, P.; Yang, S. Q.; Liu, J. Y.; Han, K. L. *Phys. Chem. Chem. Phys.* **2009**, *11*, 4385.
- (4) Matsubayashi, K.; Kubo, Y. *J. Org. Chem.* **2008**, *73*, 4915.
- (5) Rode, M. F.; Sobolewski, A. L. *Chem. Phys.* **2008**, *347*, 413.
- (6) Sobolewski Andrzej, L.; Domcke, W. *J. Phys. Chem. A* **2007**, *111*, 11725.
- (7) Yoshihara, T.; Shimada, H.; Shizuka, H.; Tobita, S. *Phys. Chem. Chem. Phys.* **2001**, *3*, 4972.
- (8) Ziółek, M.; Burdziński, G.; Karolczak, J. *J. Phys. Chem. A* **2009**, *113*, 2854.
- (9) Herbich, J.; Hung, C. Y.; Thummel, R. P.; Waluk, J. *J. Am. Chem. Soc.* **1996**, *118*, 3508.
- (10) Kyrychenko, A.; Herbich, J.; Izydorczak, M.; Wu, F.; Thummel, R. P.; Waluk, J. *J. Am. Chem. Soc.* **1999**, *121*, 11179.
- (11) Kyrychenko, A.; Herbich, J.; Wu, F.; Thummel, R. P.; Waluk, J. *J. Am. Chem. Soc.* **2000**, *122*, 2818.
- (12) Sobolewski, A. L.; Shemesh, D.; Domcke, W. *J. Phys. Chem. A* **2009**, *113*, 542.
- (13) Biczok, L.; Berces, T.; Linschitz, H. *J. Am. Chem. Soc.* **1997**, *119*, 11071.
- (14) Miyasaka, H.; Tabata, A.; Kamada, K.; Mataga, N. *J. Am. Chem. Soc.* **1993**, *115*, 7335.
- (15) Miyasaka, H.; Tabata, A.; Ojima, S.; Ikeda, N.; Mataga, N. *J. Phys. Chem.* **1993**, *97*, 8222.
- (16) Sugita, M.; Shimada, T.; Tachibana, H.; Inoue, H. *Phys. Chem. Chem. Phys.* **2001**, *3*, 2012.
- (17) Shimada, H.; Nakamura, A.; Yoshihara, T.; Tobita, S. *Photochem. Photobiol. Sci.* **2005**, *4*, 367.
- (18) Sessler, J. L.; Wang, B.; Harriman, A. *J. Am. Chem. Soc.* **1995**, *117*, 704.
- (19) Lopez Arbeloa, T.; Lopez Arbeloa, F.; Tapia, M. J.; Lopez Arbeloa, I. *J. Phys. Chem.* **1993**, *97*, 4704.
- (20) Konijnenberg, J.; Ekelmans, G.; Huizer, A.; Varma, C. *J. Chem. Soc., Faraday Trans. 2* **1989**, *85*, 39.
- (21) Tanner, C.; Manca, C.; Leutwyler, S. *Science* **2003**, *302*, 1736.
- (22) Manca, C.; Tanner, C.; Coussan, S.; Bach, A.; Leutwyler, S. *J. Chem. Phys.* **2004**, *121*, 2578.
- (23) Kwon, O.-H.; Lee, Y.-S.; Yoo, B. K.; Jang, D.-J. *Angew. Chem., Int. Ed. Engl.* **2006**, *45*, 415.
- (24) Park, S. Y.; Lee, Y. S.; Kwon, O. H.; Jang, D. J. *Chem. Commun.* **2009**, 926.
- (25) Kyrychenko, A.; Herbich, J.; Izydorczak, M.; Gil, M.; Dobkowski, J.; Wu, F. Y.; Thummel, R. P.; Waluk, J. *Isr. J. Chem.* **1999**, *39*, 309.
- (26) Nosenko, Y.; Kunitski, M.; Thummel, R. P.; Kyrychenko, A.; Herbich, J.; Waluk, J.; Riehn, C.; Brutschy, B. *J. Am. Chem. Soc.* **2006**, *128*, 10000.
- (27) Nosenko, Y.; Kyrychenko, A.; Thummel, R. P.; Waluk, J.; Brutschy, B.; Herbich, J. *Phys. Chem. Chem. Phys.* **2007**, *9*, 3276.
- (28) Nosenko, Y.; Kunitski, M.; Riehn, C.; Thummel, R. P.; Kyrychenko, A.; Herbich, J.; Waluk, J.; Brutschy, B. *J. Phys. Chem. A* **2008**, *112*, 1150.
- (29) Nosenko, Y.; Wiosna-Satyga, G.; Kunitski, M.; Petkova, I.; Singh, A.; Buma, W. J.; Thummel, R. P.; Brutschy, B.; Waluk, J. *Angew. Chem., Int. Ed. Engl.* **2008**, *47*, 6037.
- (30) Kijak, M.; Petkova, I.; Toczek, M.; Wiosna-Satyga, G.; Zielińska, A.; Herbich, J.; Thummel, R. P.; Waluk, J. *Acta Phys. Pol., A* **2007**, *112*, S105.
- (31) Mudadu, M. S.; Singh, A.; Thummel, R. P. *J. Org. Chem.* **2006**, *71*, 7611.
- (32) Krauss, O.; Brutschy, B. *Chem. Phys. Lett.* **2001**, *350*, 427.
- (33) Page, R. H.; Shen, Y. R.; Lee, Y. T. *J. Chem. Phys.* **1988**, *88*, 4621.
- (34) Brutschy, B. *Chem. Rev.* **2000**, *100*, 3891.
- (35) Frisch, M. J.; et al. *Gaussian 03*, revision B.03; Gaussian Inc.: Pittsburgh, PA, 2003.
- (36) Zhao, Y.; Truhlar, D. G. *J. Chem. Theory Comp.* **2007**, *3*, 289.
- (37) Ahlrichs, R.; Bär, M.; Häser, M.; H. H.; Kölmel, C. *Chem. Phys. Lett.* **1989**, *162*, 165.
- (38) Treutler, O.; Ahlrichs, R. *J. Chem. Phys.* **1994**, *102*, 346.
- (39) Wiosna, G.; Petkova, I.; Mudadu, M. S.; Thummel, R. P.; Waluk, J. *Chem. Phys. Lett.* **2004**, *400*, 379.
- (40) Herzberg, G. *Molecular Spectra and Molecular Structure*; van Nostrand Reinhold: New York, 1945.
- (41) Matsuda, J.; Ebata, T.; Mikami, N. *J. Chem. Phys.* **1999**, *110*, 8397.

- (42) Matsuda, J.; Ebata, T.; Mikami, N. *J. Phys. Chem. A* **2001**, *105*, 3475.
- (43) Sakai, M.; Daigoku, K.; Ishiuchi, S.; Saeki, M.; Hashimoto, K.; Fujii, M. *J. Phys. Chem. A* **2001**, *105*, 8651.
- (44) Yokoyama, F.; Watanabe, H.; Omi, T.; Ishiuchi, S.; Fujii, M. *J. Phys. Chem. A* **2001**, *105*, 9366.
- (45) Wu, R. H.; Nachtigall, P.; Brutschy, B. *Phys. Chem. Chem. Phys.* **2004**, *6*, 515.
- (46) Carney, J. R.; Zwier, T. S. *J. Phys. Chem. A* **1999**, *103*, 9943.
- (47) Matsumoto, Y.; Honma, K. *J. Chem. Phys.* **2009**, *130*, 054311.
- (48) Szydłowska, I.; Nosenko, Y.; Brutschy, B.; Tarakeshwar, P.; Herbich, J. *Phys. Chem. Chem. Phys.* **2007**, *9*, 4981.
- (49) Schiöberg, D.; Luck, W. *Spectrosc. Lett.* **1977**, *10*, 613.
- (50) Florio, G. M.; Gruenloh, C. J.; Quimpo, R. C.; Zwier, T. S. *J. Chem. Phys.* **2000**, *113*, 11143.
- (51) Kijak, M.; Waluk, J. Unpublished results.
- (52) Kyrychenko, A.; Stepanenko, Y.; Waluk, J. *J. Phys. Chem. A* **2000**, *104*, 9542.
- (53) Matsumoto, Y.; Ebata, T.; Mikami, N. *Chem. Phys. Lett.* **2001**, *338*, 52.
- (54) Destexhe, A.; Smets, J.; Adamowicz, L.; Maes, G. *J. Phys. Chem.* **1994**, *98*, 1506.
- (55) Nibu, Y.; Marui, R.; Shimada, H. *J. Phys. Chem. A* **2006**, *110*, 9627.

JP909409D